

RSC Advances

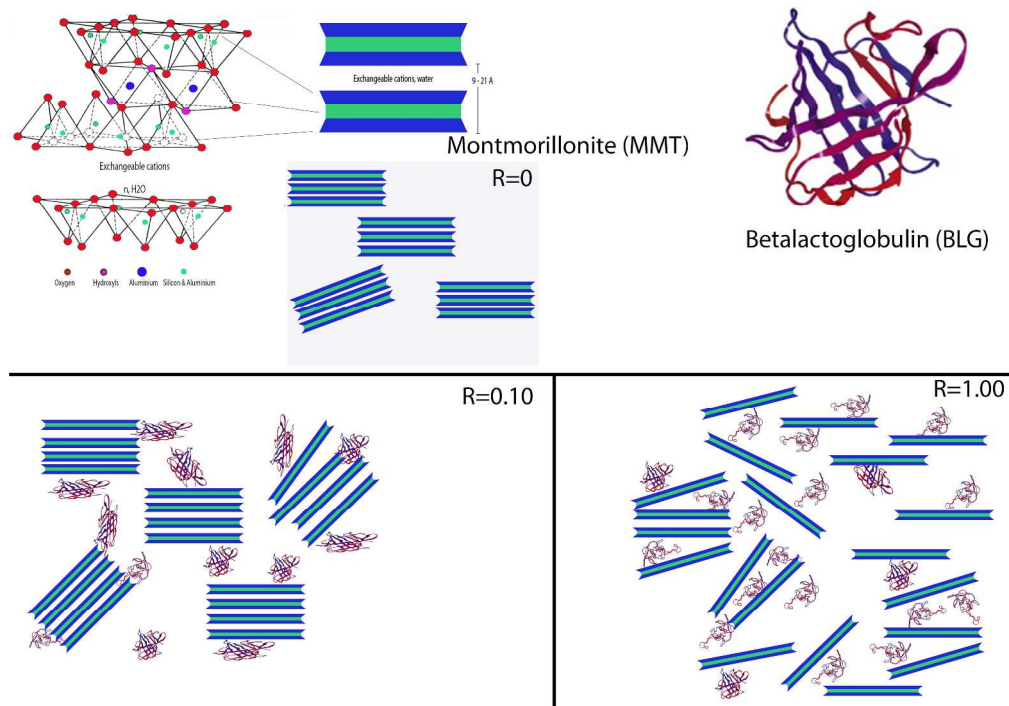


This is an *Accepted Manuscript*, which has been through the Royal Society of Chemistry peer review process and has been accepted for publication.

Accepted Manuscripts are published online shortly after acceptance, before technical editing, formatting and proof reading. Using this free service, authors can make their results available to the community, in citable form, before we publish the edited article. This *Accepted Manuscript* will be replaced by the edited, formatted and paginated article as soon as this is available.

You can find more information about *Accepted Manuscripts* in the [Information for Authors](#).

Please note that technical editing may introduce minor changes to the text and/or graphics, which may alter content. The journal's standard [Terms & Conditions](#) and the [Ethical guidelines](#) still apply. In no event shall the Royal Society of Chemistry be held responsible for any errors or omissions in this *Accepted Manuscript* or any consequences arising from the use of any information it contains.



Adsorption of betalactoglobulin on montmorillonite leads to structural changes of the protein accompanied by a partial exfoliation of clay.
297x209mm (300 x 300 DPI)

Structural studies of adsorbed protein (Betagalactoglobulin) on natural clay (Montmorillonite)

Ali Assifaoui^{(1)}, Lucie Huault⁽¹⁾, Cyrielle Maissiat⁽¹⁾, Chloé Roullier-Gall⁽¹⁾, Philippe Jeandet⁽²⁾, Jérôme Hirschinger⁽³⁾, Jésus Raya⁽³⁾, Maguy Jaber⁽⁴⁾, Jean-François Lambert⁽⁵⁾, Philippe Cayot⁽¹⁾, Régis D. Gougeon⁽¹⁾, Camille Loupiac^{(1)†}*

⁽¹⁾ UMR PAM Université de Bourgogne/AgroSup Dijon, PAM team, 1 Esplanade Erasme 21000 Dijon, France

⁽²⁾ Laboratoire de Stress, Défenses et Reproduction des Plantes, Université de Reims Champagne-Ardenne, UFR Sciences Exactes et Naturelles, Unité de Recherche Vigne et Vins de Champagne – EA 4707, B.P. 1039, Reims, cedex 02 51687, France

⁽³⁾ Institut de Chimie, UMR 7177 CNRS, Université de Strasbourg, BP 296, 67008 Strasbourg, France

⁽⁴⁾ Laboratoire d'Archéologie Moléculaire et Structurale (UMR 8220 CNRS), UPMC Université Paris 6, Tour 23-33, 4 place Jussieu, Paris, France

⁽⁵⁾ Laboratoire de Réactivité de Surface (UMR 7197 CNRS), UPMC Université Paris 6, case courrier 178, 3 R. Galilée, 94200 Ivry-sur-Seine, France

KEYWORDS

Betagalactoglobulin, Montmorillonite, Protein adsorption, Protein structural changes, Exfoliation

ABSTRACT

In this work, the adsorption of a small globular protein (betalactoglobulin, BLG), on a natural montmorillonite clay (Mt) was investigated in acidic buffer (pH=3). The combination of different characterization techniques such as zetametry, X-ray diffraction, transmission electronic microscopy, fluorescence and solid state nuclear magnetic resonance spectroscopies shed the light on the interaction mechanism between the clay mineral and the proteins. For low BLG concentration, a slight increase of the interlayer spacing of the clay mineral was noticed as well as of the structural changes of the protein. In contrast, as the concentration of BLG increased, the adsorption led to a partial exfoliation of the clay mineral, accompanied with significant secondary structural changes of the protein characterized by a loss of β -sheet organization. Altogether, our results revealed an unexpected adsorption scheme where the increase of the BLG/Mt weight ratio of the hybrid material leads to a partial exfoliation of the Mt, but at the expense of the protein native structure.

INTRODUCTION

The adsorption of proteins on clay mineral surfaces refers to very diverse processes, ranging from natural biochemistry to synthetic engineering. Such organic-inorganic interactions are indeed at the basis of various microbially driven processes in soil organic matter and are even considered as being relevant to prebiotic processes involving catalytic reactions between amino acid building blocks and clay surfaces.^{1, 2} Alternatively and along with the advent of nanotechnologies, many studies have focused on macromolecule layered silicate interactions for the design of advanced hybrid materials with applications in fields as diverse as catalysis or wine fining and food processing.³⁻⁶

A particular interest of protein-clay systems – or more general protein-porous materials – concerns their ability to simulate confined environments for structural biology approaches.⁷⁻⁹ While macroscopic descriptions of the phenomena provide interesting information it is felt that a molecular-level investigation of the interaction between clay layers and proteins will be essential for a rational improvement of desired properties.^{8, 10} Therefore, the attention to spectroscopic characterization of these systems has been growing. However, such approaches are often complex and their detailed analysis can be more easily achieved by using model systems.

Beta-lactoglobulin (BLG) is a model close-packed and well-ordered protein. BLG is one of the major components of whey protein from bovine milk and belongs to the lipocalin family which is known for specific transporter activity.¹¹ This globular protein, which is easily isolated from raw milk,¹² exhibits 162 residues and a molecular weight of 18.4 kDa. A structural particularity relies on its core made up of a short α -helix segment and eight strands of antiparallel β sheets, which wrap round to form a conical barrel. However, the quaternary

structure is both concentration and pH-dependant and the monomeric form of BLG exists below pH 3. X-ray crystallography and small-angle X-ray scattering studies have revealed that the BLG dimer is an approximately prolate ellipsoid with a length of 6.9 nm and a width of 3.6 nm.¹¹ Alternatively the dimer can be described by two impinging spheres with a radius of 1.8 nm.¹¹ BLG has a hydrophobic binding site in its interior, but also a weaker one on its exterior, which bind to various hydrophobic ligands, mainly retinol and long-chain fatty acids.

Bentonite – a naturally occurring montmorillonite – type phyllosilicate is widely employed in environmental processes such as waste water treatments and in industrial processes such as clarification of wines and adsorbent for oil-substances.¹³⁻¹⁵ Montmorillonites display a layered structure formed by two sheets of tetrahedrally coordinated silicon linked through a sheet of octahedrally coordinated aluminum. Due to intralayer octahedral (and to some extent tetrahedral) substitutions, montmorillonites exhibit an overall negative basal surface charge that is balanced by interlayer cations (mostly calcium, magnesium or sodium). However, if this surface charge is pH-independent and provides an electronegative charge to montmorillonite, it is established that layer edges also exhibit reactive pH-dependent charged sites due to the protonation / deprotonation of silanol groups.¹⁶

Adsorption of proteins onto montmorillonites can proceed from various mechanisms of interaction involving either basal surface planes or edge sites or both, bearing in mind that protein's structure and charge also govern their adsorption.^{8, 17} At pH below their isoelectric points (iep), proteins are positively charged and their adsorption on clay mineral would basically be explained in terms of electrostatic interactions. However, whether such interactions involve edge sites or basal planes remains unclear. If several authors report on the partial or total intercalation of BSA¹⁸⁻²⁰ or polylysine^{21, 22} within interlayers as witnessed by X-ray d_{001} basal spacing increase for instance, other authors have shown that kaolinite – a

non-swelling clay – is also a strong adsorbent for proteins; indicating that protein molecules were immobilized only at external surfaces and edges of the kaolinite.¹⁰ In these studies, electrostatic interactions between hydrophilic regions of the clay and protein polar aminoacyl residues dominated the adsorption process. However, protein adsorption on montmorillonite is generally assumed to be maximum at pH values near their iep or higher^{19, 23-26} and even high ionic strengths do not necessarily prevent adsorption.²³ Likewise, Kolman and co-workers showed recently that when a protein mixture was pumped through a montmorillonite bed, adsorption was not driven by lysozyme (iep nearly 9.5) – the only protein bearing a net positive charge under their experimental conditions– but instead was the result of synergistic effects between the different proteins in mixture.²⁷ Therefore, mechanisms other than electrostatic interactions have to be considered and hydrogen bonding and/or hydrophobic interactions between protein apolar amino acids and siloxane layers (or other protein fragments) may contribute to the adsorption process.^{23, 28}

Another important feature related to the adsorption of proteins on solid surfaces in general and montmorillonite in particular, concerns the structural modifications of both the organic and the inorganic polymers, and various results dealing with these aspects are also reported in the literature. Fourier Transform Infra-Red spectroscopy (FTIR) and enzymatic studies for instance, have emphasized pH-dependent modification and/or orientation of adsorbed enzymes, characterized by protein structural unfolding due to electrostatic interactions.^{7, 29} But recently, Helassa and co-workers showed that the *Bacillus thuringiensis* (*Bt*) (Cry1 Aa) toxin monomer was adsorbed in its native state whereas only the quaternary structure of the oligomer was barely modified.²³ Protein structure integrity is of basic importance for their possible remnant activity in the adsorbed state and it is the adsorption without structural modification that could explain the conservation of insecticidal activity of Cry toxins in soils.²³

Similarly, nanohybrids formed by the adsorption of lysozyme on montmorillonite were considered to keep antibacterial properties pertaining to the macromolecule, thus allowing the synthesis of new biofunctional hybrid materials.³⁰ The same authors further showed that such nanohybrids do arise from the exfoliation of montmorillonite by protein mixtures leading to stacked platelets separated by gaps of the order of 3.5-4.5 nm.²⁷ However, Lin and co-workers reported recently that BSA could be entirely intercalated within layered silicates – though not talking about exfoliation – with silicate *d* spacings ranging from 2.1 to 6.2 nm according to the BSA/Na⁺-Mt weight ratio.²⁰ Interestingly for the lowest *d* spacings, these authors indicated that BSA molecules (estimated size of 4x4x14 nm³) were embedded in a compressed conformation.²⁰ Thus, all these results emphasize the need for a better understanding of mechanisms at the protein-clay interfaces with improved definitions of boundaries between adsorption, intercalation and exfoliation along with corresponding structural modifications of the interacting proteins. Indeed, although hydrodynamic radii of many proteins in solution are theoretically too high to allow for a complete intercalation within interlayer spaces – while keeping the structural integrity of the clay mineral as is the case for the adsorption of small cationic elements – both molecular simulations and adsorption experiments acknowledge the fact that proteins could be entirely intercalated through an extensive unfolding or a compressed conformation within a 1.4 to 2.3 nm-large interlayer space.^{31, 32}

Here, we report on the adsorption of betalactoglobulin on montmorillonite in conditions favoring electrostatic interactions between montmorillonite and the monomeric form of BLG (pH=3). As indicated above, it is indeed well known that at room temperature, neutral pH and physiological conditions, the BLG is in a dimeric state, while at pH=3 and concentration below 2 g.L⁻¹, the monomeric form is predominant and the protein is positively charged.

Complementary approaches were thus used to quantify the protein adsorption, to characterize the organic-inorganic interface and to assess structural modifications of the adsorbed protein monomer.

MATERIALS AND METHODS

Materials

Betalactoglobulin (BLG). BLG was purified from whey powder (Bipro from Danisco), following a procedure already detailed elsewhere, that not only allows the production of high amounts of BLG, but more importantly in its native form.^{33, 34} Briefly, the powder was first suspended in deionized water under stirring for 2 hours to obtain a protein concentration close to 20 g.L⁻¹. Then, trichloroacetic acid (3% w/v) was added to the suspension to lower the pH to pH=2, allowing the precipitation of all the proteins in the suspension excepting the BLG. The precipitate was removed by centrifugation at 12000 g for 30 min. The supernatant was collected, and extensively dialyzed against water and then against Mc Ilvaine buffer (0.1 M citric acid and 0.2 M sodium phosphate dibasic, pH=3). The concentration of BLG stock's solution was determined from the absorbance of the solution at 278 nm, using the specific extinction coefficient of 0.96 L.g⁻¹.cm⁻¹. For the adsorption's experiments, this BLG stock's solution was diluted in Mc Ilvaine buffer to obtain final concentrations going from 0.1 to 1.0 g.L⁻¹.

Montmorillonite (Mt). Sodium-activation of the natural clay mineral used here has already been reported elsewhere.³⁵ For this study and in order to obtain a purified fraction of montmorillonite (Mt), this sodium-activated bentonite was treated by both ultrasonic and sedimentation procedures.³⁶ The mineral was ground using a manual mortar and sieved to 125 µm. Five grams of sieved powder were suspended for 30 minutes in 1 L of deionized

water. The suspension was sonicated for 20 minutes, stirred for 24 h, sonicated again for 20 min and centrifuged at 3000 g for 10 minutes. The supernatant was collected and dried in an oven at 105 °C until complete water evaporation. Sediments composed mainly by quartz were then eliminated. X-ray diffraction patterns (data not shown) of both raw and purified minerals showed an important increase in the intensity ratio of the two characteristic reflections (I_{Mt}/I_{quartz}) for the purified bentonite indicating the efficiency of the purification.

Adsorption of BLG on the purified montmorillonite

Adsorption experiments were carried out by direct contact between the Mt suspension in Mc Ilvaine buffer (pH=3) at a fixed concentration of 1 g.L⁻¹ and BLG solutions – in the same buffer– of concentrations ranging from 0 to 1 g.L⁻¹. The adsorption experiments were done under continuous stirring at low temperature (T=4 °C) to avoid protein denaturation and bacterial growth. The equilibrium was reached after 20 hours of contact. Samples were then centrifuged at 12000 g for 10 minutes. Both supernatants and pellets were collected and analyzed. Pellets were washed with water to remove loosely sorbed proteins. Each analysis was performed in triplicate. The remaining amount of BLG in the supernatant was determined by UV spectrometry at 278 nm. The amount of adsorbed BLG was calculated by the difference between the initial concentration of BLG and the remaining concentration in the supernatant. The pellet was dried at room temperature and then kept at a water activity close to zero using P₂O₅ powder as a dehydrating agent. The amount of adsorbed protein per unit mass at equilibrium was calculated with equation 1:

$$q_e = \frac{V \times (C_0 - C)}{m} \quad (\text{Eq. 1})$$

Where C_0 and C are the BLG initial and equilibrium concentrations, respectively (mg.L⁻¹); V , the volume of the suspension (L) and m , the Mt weight (g).

Characterization methods

Fluorescence spectroscopy. The BLG intrinsic fluorescence in both the supernatant and the pellet fractions was determined using a LS50B (Perkin-Elmer) Fluorescence spectrophotometer. The measurements were performed in a 1 cm quartz cell at 25 °C for the supernatant and with a solid sample holder accessory for front face measurement for the pellet. Emission spectra were recorded from 295 to 500 nm with an excitation wavelength of 280 nm. The spectral resolution was 5 nm. Betalactoglobulin contains two Tryptophan (Trp) residues, Trp-19 and Trp-61, which are in different environments. Trp-19 is in an apolar environment within the hydrophobic cavity, whereas Trp -61 is partly exposed to the aqueous solvent. The recorded signal is thus an average of the signal linked to these two tryptophans.

X-ray diffraction (XRD). The crystalline structure of clay minerals before and after adsorption (dried pellet) was studied by XRD with a Siemens D5000 powder X-ray diffractometer, using the $\text{CuK}\alpha$ ($\lambda = 1.5406 \text{ \AA}$) radiation and an INEL CPS 120 curved detector. X-ray patterns were recorded in the 2θ range 3–60 deg. with a scan rate of $0.5 \text{ deg. min}^{-1}$.

Transmission electron microscopy (TEM). Micrographs were recorded on a JEOL JEM-100 CXII apparatus operating at 200keV. To prepare the sample a few milligrams of the sample are mixed in a Beem capsule with Agar 100 embedding resin. After polymerization at 60 °C overnight, the blocks are cut using a microtome equipped with a diamond knife. The ultra-thin slices about 50 nm, are recovered on copper grids and examined.

Surface electrical charges. Electrophoretic mobility measurements were done using a ZetaCompact instrument (Cad instrumentation, France). Electrophoretic mobilities were calculated from the displacement of particles subjected to a constant direct-electric current field of 800 V.m^{-1} .

Nuclear magnetic resonance (NMR). ^1H - ^{13}C Cross-Polarisation Magic Angle Spinning (CP-MAS) NMR experiments were run on a Bruker DSX 300 spectrometer operating at frequencies of 300.1 MHz and 75.5 MHz for ^1H and ^{13}C , respectively. All the spectra were acquired with a Bruker double-channel 4 mm MAS probe at spinning speeds of 10 kHz. The ^1H - ^{13}C CP-MAS spectra were obtained by cross-polarization, with spinal 64 proton dipolar decoupling. Hartmann-Hahn matching for the ^1H - ^{13}C CP-MAS experiments was set on adamantane for ^1H and ^{13}C radio-frequency fields of ca. 60 kHz. Chemical shifts for ^1H and ^{13}C spectra were referenced to the signal of water (4.87 ppm) and to the methylene signal of adamantane (29.47 ppm), respectively. Other experimental details are indicated in the figure captions.

RESULTS AND DISCUSSION

Adsorption and interface characterization

The adsorption isotherm of BLG on the Mt mineral (Figure 1) displays a classical Langmuir-like shape already observed for the adsorption of other proteins on montmorillonite.¹⁷ Such isotherm is characterized by a saturation point beyond which a plateau value is obtained for the adsorbed concentration. One could apply the Langmuir model to our experimental points, using the classical equation 2:

$$C_e/C_{ads} = 1/(C_{ads}^S K) + C_e/C_{ads}^S \quad (\text{Eq. 2})$$

Where C_e is the equilibrium concentration of BLG; C_{ads} , the adsorbed amount of BLG (mg.g^{-1}) at any equilibrium concentration C_e ; and C_{ads}^s , the adsorbed amount of BLG (mg.g^{-1}) at saturation; K is a numerical expression of the affinity of BLG for the Mt (the higher the value, the higher the affinity).

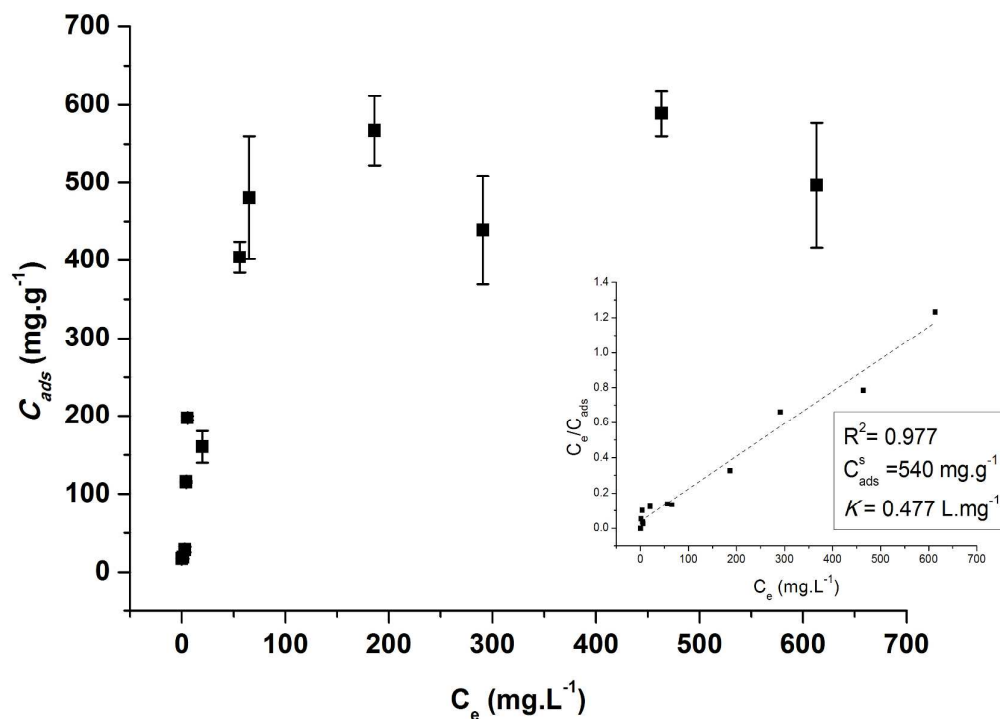


Figure 1: Variation of adsorbed BLG (mg.g^{-1} of clay) with the initial BLG concentration (mg.L^{-1}); Mt suspension = 1.0 g.L^{-1} . Adsorption isotherm was realized in Mc Ilvaine buffer ($\text{pH}=3$) and at $T=4 \text{ }^\circ\text{C}$. Inset is Langmuir presentation according to the equation 2.

From this model, C_{ads}^s and K values were equal to 540 mg.g^{-1} and 0.477 L.mg^{-1} , respectively, which witnesses to a high affinity of BLG for the Mt.¹⁷ The high adsorption capacity C_{ads}^s indicated a high degree of irreversibility of the adsorption system.³⁷ The relative affinity of BLG for adsorption may be evaluated with the help of numerical values of K . According to

the literature, the K value for the adsorption of hemoglobin onto bentonite mineral was about $0.15 \times 10^6 \text{ L.mol}^{-1}$, whereas for the adsorption of casein onto alkali-treated bentonite mineral it was about $0.18 \times 10^6 \text{ L.mol}^{-1}$.^{17, 38} In the present study, the K value was found to be 0.477 L.mg^{-1} which corresponds to $0.87 \times 10^6 \text{ L.mol}^{-1}$. This value is about 6 times higher than that observed for hemoglobin and casein which implies that BLG is much more prone for adsorption. For the following, analyses were focused on three BLG concentrations (0.10, 0.25 and 1.00 g.L^{-1}). The amount of the Mt was maintained to 1 g.L^{-1} . The BLG/Mt ratio was then equal to 0.10, 0.25 and 1.00, respectively. Hybrid composites will then be referred to as BLG-Mt-0.10, BLG-Mt-0.25 and BLG-Mt-1.00.

The electrical surface charges of Mt and BLG solutions within the 2-8 pH range was measured by zetametry (Figure 2). Results showed that the global surface charge of MT was negative whatever the pH of the suspension. As the pH increased, this global charge became more negative and reached a minimum value of $-2.5 \mu\text{m.cm.s}^{-1}.\text{V}^{-1}$ at pH=7, due to the contribution of the pH-dependent edge charges of the clay mineral. At pH=3, which corresponds to our experimental conditions (Mc Ilvaine buffer), the global charge for the Mt suspension was negative with an electrophoretic mobility of $-1.82 \mu\text{m.cm.s}^{-1}.\text{V}^{-1}$ (Figure 2). The net surface charge of BLG is positive under acidic conditions and negative under neutral and alkaline conditions. At pH=3, the BLG presented a positive charge with an electrophoretic mobility of $0.5 \mu\text{m.cm.s}^{-1}.\text{V}^{-1}$. It is important to note that under our experimental conditions, both the BLG and the Mt edges were positively charged, while the Mt basal surface exhibited an overall negative charge density.

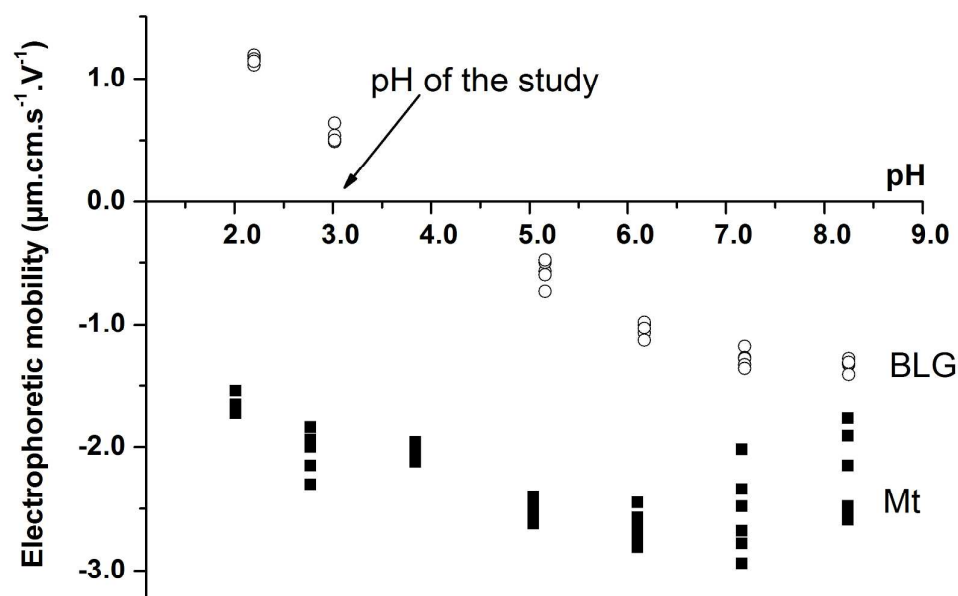


Figure 2: Electrophoretic mobility of clay suspension and BLG solution as a function of pH.

The electrophoretic mobility of the three BLG-Mt composites was also measured (Table 1). As the concentration of BLG increased (BLG-Mt ratio increased), the electrophoretic mobility – negative and equal to $-2.09 \mu\text{m.cm.s}^{-1}.\text{V}^{-1}$ for the BLG-Mt-0.10 composite – increased and became positive and equal to $0.8 \mu\text{m.cm.s}^{-1}.\text{V}^{-1}$ for the BLG-Mt-1.00 composite. These results show that for low BLG concentrations in contact with Mt (ratios 0.10 and 0.25), interactions between BLG and Mt did not entail all of the basal negative charges. For higher BLG concentration (BLG-Mt-1.00), the global charge was positive and close to the one observed for the protein. One can conclude that at low protein concentration, the surface charge properties of the clay-protein material is driven by the clay charge whereas at high protein concentration it is driven by the protein charge.

Table 1: Electrophoretic mobility for Mt and BLG suspensions and for hybrid composites at the three ratios studied at pH=3.

	Mt	BLG-Mt			BLG
		0.10	0.25	1.00	
Electrophoretic mobility ($\mu\text{m.cm.s}^{-1}.\text{V}^{-1}$)	-2.09±0.20	-2.27±0.05	-1.95±0.07	0.82±0.07	0.52±0.05

Mineral structure upon adsorption

The crystalline structures of the purified Mt and the different BLG-Mt composites were studied by X-Ray Diffraction (XRD) (Figure 3). For the Mt sample, the X-ray diffraction patterns exhibited characteristics of dioctahedral smectite clay minerals. The smectite phase was clearly identified by (*hkl*) reflections at 19.7° (020, 110) and 35.3° (130, 200). The angular position of the (060) reflection at 62° (0.15 nm) indicated the predominance of dioctahedral domains in the octahedral sheets of the homoionic Mt.^{39, 40} It was observed that the other characteristic bands of montmorillonite were unchanged upon adsorption for all of the composites, therefore confirming that the structure within each Mt layer remained intact. The Mt d_{001} value (basal spacing) was about 1.3 nm. Taking into account the thickness of a layer (0.97 nm), this corresponds to the “one-water layer” hydration state of the interlayer cations (the thickness of one water layer being about 0.25 nm). At low concentration of BLG (0.1 g.L⁻¹), the typical d_{001} diffraction peak for BLG-Mt-0.10 shifted from 6.8° (basal spacing 1.3 nm) to 5.9° (basal spacing 1.5 nm). As can be seen from figure 3, an increase of the diffracted intensity appeared at low 2θ values (<3°). This increase was due to the second order of a (001) reflection peak expected at lower 2θ. It is noted that at 2θ=3°, the corresponding interlayer distance should be about 3.0 nm. As the amount of BLG increased (0.25 and 1.0 g.L⁻¹), the intensity of the d_{001} peak at 1.5 nm decreased while the <3° peak

increased, indicating that only a fraction of Mt remained with the initial interlayer space, whereas an increasing fraction with exfoliation-like characteristics would appear. As a consequence, we can consider that with the increasing of the BLG concentration, different populations of layers were observed : non-intercalated one (1.3 nm), and intercalated layers (3 and 1.5 nm). As the peak intensity is very low we can not conclude on the degree of intercalation or the presence of exfoliated layers. These results will be supported by TEM analyses.

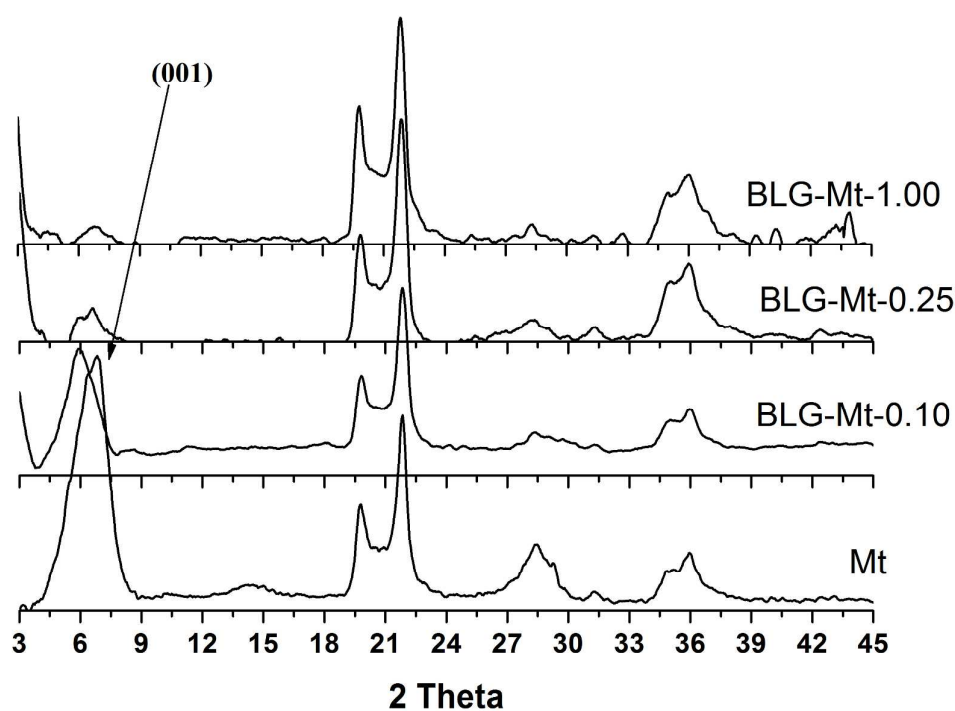


Figure 3: X-ray diffractograms of Mt and BLG-Mt composites

To additionally clarify the XRD results, the same samples were analysed using TEM. The densitometric cross-section of BLG-Mt-0.10 particle view along the A-A profile (Figure 4) showed regular stratification with a characteristic average length of 1.2 ± 0.2 nm – close to

the value obtained by XRD ($d = 1.5$ nm). For higher amounts of adsorbed BLG (BLG-Mt-1.00), the TEM micrographs indicated that the periodicity of montmorillonite platelets within particles was partly lost, thus suggesting exfoliation of Mt. A large number of primary aggregates remained with BLG-Mt-0.10 characteristics. This was confirmed by the small diffraction peak observed by XRD at 5.9° (Figure 2). It was also noted that the interlayer space is increased to around 2.4 – 3.5 nm as shown by the densitometric analysis (the linear cross-section B-B, figure 4). Kolman and co-workers have observed also an exfoliation at $0.6 \text{ g} \cdot \text{g}^{-1}$ (proteins: Mt ratio) when ovotransferrin and albumins were adsorbed to Mt.²⁷ Chen and co-workers have found that soy protein intercalate and exfoliate layered Na-Mt.²⁸ Their explanation considered at least two types of interactions, surface electrostatic interaction and hydrogen bonding. In the present study, TEM and XRD results indicate that at low BLG concentration, the adsorption of the protein keeps the organization of the Mt interlayer. While for high BLG concentration, the adsorption causes partial exfoliation.

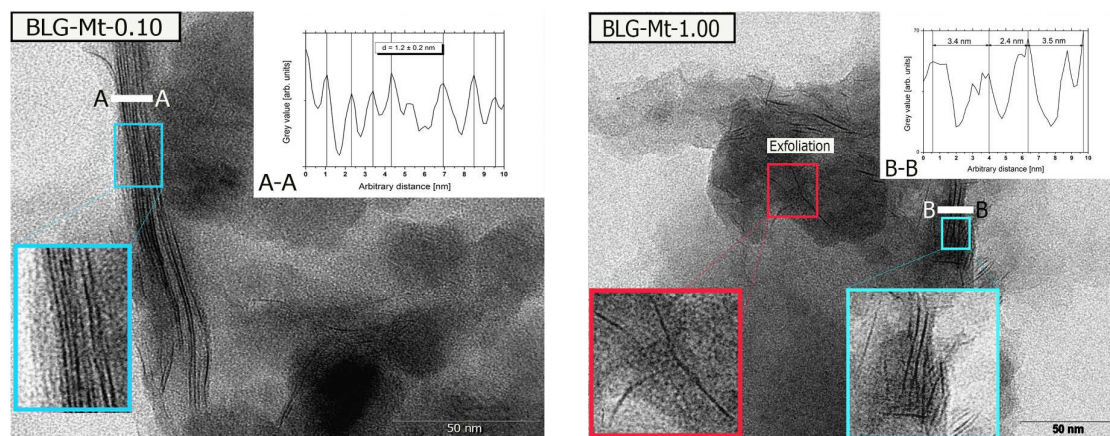


Figure 4: Transmission electron micrographs (TEM) of hybrid composites for low ($0.10 \text{ g} \cdot \text{L}^{-1}$ left) and high ($1.00 \text{ g} \cdot \text{L}^{-1}$ right) BLG concentrations respectively. Insets show densitometric profiles of particle images measured along A-A and B-B lines respectively.

Protein structure upon adsorption

Tryptophan fluorescence spectroscopy was used to study the structure of both adsorbed and non-adsorbed proteins (in the supernatant). At equilibrium, BLG-Mt suspensions were centrifuged and both the supernatants and pellets were collected for measurements (Figure 5a and 5b respectively). The spectra for supernatants (Figure 5a) confirmed that for the two lowest BLG-Mt ratios (BLG-Mt-0.10 and BLG-Mt-0.25), the protein was completely adsorbed. Indeed for these ratios, no emission bands were observed (in comparison with the BLG solution). In contrast, the spectrum for the highest ratio (R=1.00) appeared to be very similar to that of the protein alone. The position of the emission maximum (λ_{max}) was found around 338 nm as previously observed in the literature.^{41, 42} This confirmed that for this ratio, the Mt binding sites were saturated (since non-adsorbed proteins were consistently found in the supernatant). This also indicates that there were no changes in the structure of these proteins which remained in solution. For the hybrid composites (Figure 5b), an increase of the fluorescence emission intensity going from the lowest ratio to the highest was observed. This again confirmed the increase of the quantity of adsorbed protein. Moreover the position of the emission maxima for the adsorbed proteins shifted to highest wavelengths (around 5 nm), indicating that the tryptophan residues environments became more polar. These results clearly show that as the adsorbed BLG concentration increased, the structural changes of the protein also increased. Although out of the scope of this study, it is important to note that these structural changes in the protein would certainly modify the protein ability to bind various hydrophobic ligands, such as resveratrol⁴² and long-chain fatty acids.

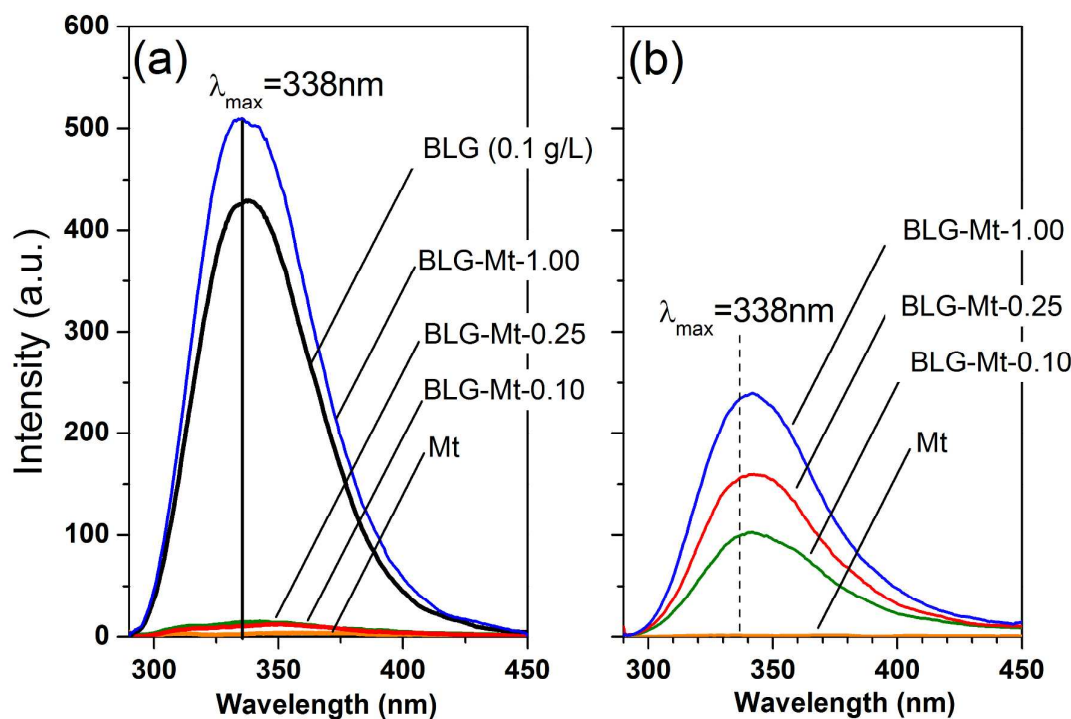


Figure 5 : Fluorescence emission spectra of BLG tryptophan in the supernatant (a) and in the pellets (hybrid composites) (b). The excitation wavelength was 280 nm.

Further indications of the betalactoglobulin structural modifications upon adsorption could be drawn from ^1H - ^{13}C CP-MAS NMR experiments. Figure 6 shows the ^1H - ^{13}C CP-MAS spectra of BLG and BLG-Mt-1.00, which display similar spectra characterized by an intense peak around 173 ppm for backbone carbonyls, four peaks between 160 and 110 ppm assigned to aromatic side chain carbons, including in particular the C_ξ from Tyr and Arg residues at 155 ppm⁴³, the peak at about 52 ppm corresponding to backbone α -CH carbons, and three other peaks between 50 and 0 ppm attributed to aliphatic side-chain carbons. ^1H - ^{13}C CP-MAS spectra of polypeptides and proteins have proven to be useful (and semi-quantitative) indicators of local structural features at the atomic size range.¹³

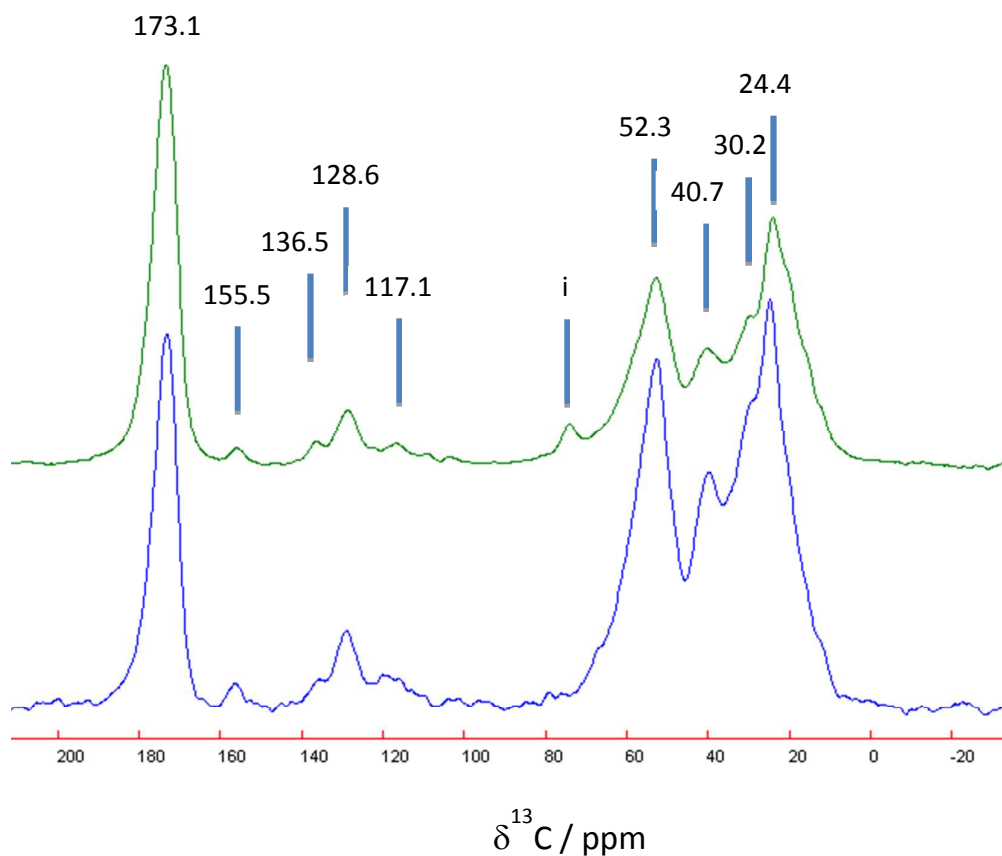


Figure 6: ^1H - ^{13}C CP-MAS NMR spectra of lyophilized BLG powder (bottom) and BLG-Mt-1.00 (top); Contact time = 1 ms; Number of transients = 2800 (BLG) and 14648 (BLG-Mt-1.00); Recycling time = 4 s; i : impurity.

Such features can be drawn from spectral parameters (chemical shifts and linewidths) derived from the deconvoluted spectra (Figure 7) as illustrated by components attributed to carbonyl and α -CH carbons. The carbonyl peak could be deconvoluted into two components associated with β -sheet secondary structures (lower frequency corresponding to the main structure in BLG) and together α -helix and random coil structures (higher frequencies corresponding to the average of minor parts in BLG) (Figure 7a). Such deconvolution led to relative proportions of 75 and 25% for the β -sheet and helix-coiled components, respectively, which is

in rather good agreement with known secondary structural features for betalactoglobulin.¹¹ A semi-quantitative indication of the impact of the adsorption on the BLG structure could be obtained from the evolution of the helix-coiled / β -sheet ratio (peak areas ratio) (Figure 7b). For a low BLG concentration (BLG-Mt-0.10), both the carbonyl chemical shifts (Figure 7A) and β -sheet/helix-coiled ratio (Figure 7b, Table 2) increased, compared to pure BLG. At this low ratio a small structural modification in the BLG structure may occur, which would be characterized by local disordering of β -sheets in particular (increase of the carbonyl low frequency component from 172.6 ppm to nearly 173 ppm, Figure 7a). Actually, this disordering seemed to be a reorganization among secondary structures, with a slight increase of the β -sheets proportion relative to the coils (Figure 7b). As the initial BLG concentration increased, one can progressively observe a shift in the chemical shifts towards lower frequencies (Figure 7a) and a significant decrease of β -sheet/helix-coiled ratio (Figure 7b). Clearly, these results demonstrate that the adsorption process does not follow a linear trend with the increase of the BLG concentration. Two different interaction mechanisms are involved for low (BLG-Mt-0.10) and high (BLG-Mt-1.00) ratios, with a transition between both, that already operates below the intermediate BLG-Mt-0.25 ratio.

In contrast with the low BLG:Mt ratio, both the intermediate and the high ratio appeared to be characterized by a significant decrease of the relative proportion of β -sheets (Figure 7b), and thus a disordering which is consistent with the fluorescence results.

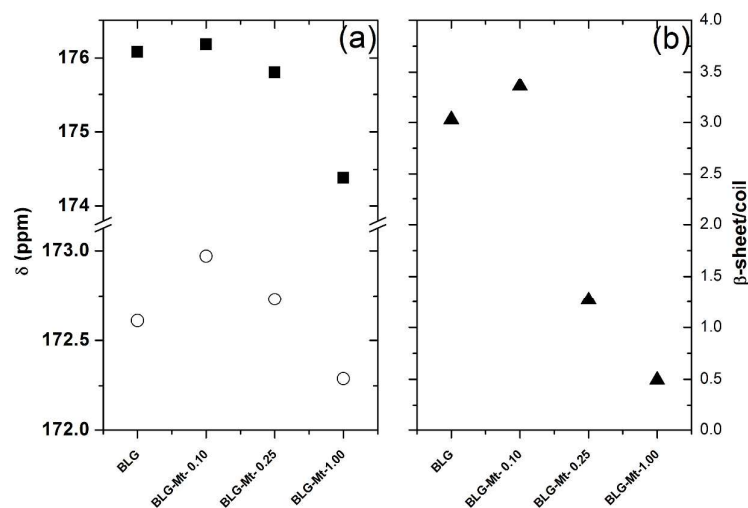


Figure 7: Evolution for BLG and BLG-Mt composites (a) of carbonyl ^{13}C chemical shifts for the two deconvoluted components in Table 2 (dark squares and empty circles correspond to coils and β -sheets structure, respectively), and (b) of the ratio of the carbonyl β -sheet component peak area to the coiled component peak area (β -sheet/coiled)

Table 2: Chemical shifts (δ) and linewidths (Δ) of deconvoluted components for both carbonyl and α -CH carbons

		Carbonyl		α -CH	
		Coils	β -sheets	Coils	β -sheets
BLG	δ (ppm)	176.1	172.6	58.0	52.3
	Δ (ppm)	6.6	5.7	12.1	7.8
BLG-Mt-0.10	δ (ppm)	176.2	173.0	59.6	52.7
	Δ (ppm)	5.1	6.5	15.1	7.8
BLG-Mt-0.25	δ (ppm)	175.8	172.7	59.0	52.6
	Δ (ppm)	8.0	5.4	14.7	8.0
BLG-Mt-1.00	δ (ppm)	174.4	172.3	56.0	52.3
	Δ (ppm)	7.5	5.1	15.7	7.1

CONCLUSION

The adsorption of beta-lactoglobulin (BLG) on montmorillonite (Mt) at pH=3 was found to be dependent of the BLG concentration. Regarding the structure of Mt, a slight modification of the interlayer space of the clay mineral was observed for low protein concentrations as witnessed by XRD and TEM. Moreover, the global charge (as observed by electrophoretic mobility) of the hybrid composite remains negative and constant indicating that the mechanism of interaction is driven by the clay charge. For the highest protein concentration (BLG-Mt-1.00), a partial exfoliation of montmorillonite was observed on TEM micrographs. This exfoliation could explain the global positive charge observed for this ratio. Furthermore, the adsorbed BLG exhibits a structural conformation different from the BLG alone. Tryptophan (Trp) residues present in the protein are affected by the adsorption as shown by fluorescence spectroscopy (a shift of +5 nm is observed at low ratios). Indeed, the BLG adsorption shifted tryptophan residues to a more polar environment. Finally, NMR results further showed that this change of tryptophan residues environment can be linked to a progressive loss of β -sheet secondary structures. One can thus conclude that the secondary structure of the protein is affected by the adsorption. Altogether, our results revealed a surprising adsorption scheme where the increase of the BLG/Mt weight ratio of the hybrid material leads to a partial exfoliation of the Mt, but at the expense of the protein native structure

ACKNOWLEDGEMENTS

This work was financially supported by the Region Bourgogne and the Bureau Interprofessionel des Vins de Bourgogne. Authors would like to thank Miss Bernadette

Rollin, Miss Marie-Laure Leonard and Jean-Marc Dachicourt for their technical helps (protein purification and XRD, respectively).

AUTHOR INFORMATION

Corresponding Author: Telephone : + 33380393214. Email: ali.assifaoui@u-bourgogne.fr

† AUTHOR CONTRIBUTIONS:

AA, PC, JFL, RDG and CL designed research; LH, CM, CRG, JH, JR, JFL and MJ performed research; AA, LH, RDG and CL analyzed data; AA, RDG and CL wrote the paper; PJ, MJ, AA, RDG and CL reviewed and edited the paper.

REFERENCES:

1. H. Quiquampoix and R. G. Burns, *Elements*, 2007, **3**, 401-406.
2. J.-F. Lambert, *Orig Life Evol Biosph*, 2008, **38**, 211-242.
3. A. E. Sommer, G. Fetter, P. Bosch and O. Novelo, *Polym. Adv. Technol.*, 2011, **22**, 2638-2642.
4. M. Reger, T. Sekine and H. Hoffmann, *Colloid. Polym. Sci.*, 2012, **290**, 631-640.
5. A. T. T. Tran, D. A. Patterson and B. J. James, *J. Food Eng.*, 2012, **112**, 38-49.
6. A. L. Laza, M. Jaber, J. Miehe-Brendle, H. Demais, H. Le Deit, L. Delmotte and L. Vidal, *Journal of nanoscience and nanotechnology*, 2007, **7**, 3207-3213.
7. S. Servagent-Noinville, M. Revault, H. Quiquampoix and M. H. Baron, *J. Colloid Interface Sci.*, 2000, **221**, 273-283.
8. S. Balme, R. Guegan, J.-M. Janot, M. Jaber, M. Lepoitevin, P. Dejardin, X. Bourrat and M. Motelica-Heino, *Soft Matter*, 2013, **9**, 3188-3196.
9. J. Deere, E. Magner, J. G. Wall and B. K. Hodnett, *J. Phys. Chem. B*, 2002, **106**, 7340-7347.
10. S. Barral, M. A. Villa-García, M. Rendueles and M. Díaz, *Acta Mater.*, 2008, **56**, 2784-2790.
11. G. Kontopidis, C. Holt and L. Sawyer, *J. Dairy Sci.*, 2004, **87**, 785-796.
12. K. K. Fox, V. H. Holsinger, L. P. Posati and M. J. Pallansch, *J. Dairy Sci.*, **50**, 1363-1367.
13. V. L. Fernandez, J. A. Reimer and M. M. Denn, *J. Amer. Chem. Soc.*, 1992, **114**, 9634-9642.
14. J. De Bruijn, C. Loyola, A. Flores, F. Hevia, P. Melín and I. Serra, *Int. J. Food Sci. Technol.*, 2009, **44**, 330-336.
15. K. F. Pocock, F. N. Salazar and E. J. Waters, *Aust. J. Grape Wine Res.*, 2011, **17**, 280-284.
16. R. L. Sanders, N. M. Washton and K. T. Mueller, *J. Phys. Chem. C*, 2010, **114**, 5491-5498.
17. A. K. Bajpai and R. Sachdeva, *J. Appl. Polym. Sci.*, 2002, **85**, 1607-1618.
18. M. Lepoitevin, M. Jaber, R. Guégan, J.-M. Janot, P. Dejardin, F. Henn and S. Balme, *Appl. Clay Sci.*, 2014, **95**, 396-402.
19. A. De Cristofaro and A. Violante, *Appl. Clay Sci.*, 2001, **19**, 59-67.
20. J. J. Lin, J. C. Wei, T. Y. Juang and W. C. Tsai, *Langmuir*, 2007, **23**, 1995-1999.
21. R. D. Gougeon, M. Reinholdt, L. Delmotte, J. Miehe-Brendle, J. M. Chezeau, R. Le Dred, R. Marchal and P. Jeandet, *Langmuir*, 2002, **18**, 3396-3398.
22. R. D. Gougeon, M. Soulard, M. Reinholdt, J. Miehe-Brendle, J. M. Chezeau, R. Le Dred, R. Marchal and P. Jeandet, *Eur. J. Inorg. Chem.*, 2003, 1366-1372.
23. N. Helassa, M. Revault, H. Quiquampoix, P. Dejardin, S. Staunton and S. Noinville, *J. Colloid Interface Sci.*, 2011, **356**, 718-725.
24. A. Kondo, S. Oku and K. Higashitani, *J. Colloid Interface Sci.*, 1991, **143**, 214-221.
25. A. Kondo, S. Oku, F. Murakami and K. Higashitani, *Colloid. Surf. B.*, 1993, **1**, 197-201.
26. H. Quiquampoix and R. G. Ratcliffe, *J. Colloid Interface Sci.*, 1992, **148**, 343-352.
27. K. Kolman, W. Steffen, G. Bugla-Ploskonska, A. Skwara, J. Piglowski, H. J. Butt and A. Kiersnowski, *J. Colloid Interface Sci.*, 2012, **374**, 135-140.

28. P. Chen and L. Zhang, *Biomacromolecules*, 2006, **7**, 1700-1706.
29. H. Quiquampoix, S. Staunton, M. H. Baron and R. G. Ratcliffe, *Colloid. Surf. A.*, 1993, **75**, 85-93.
30. V. Krisdhasima, P. Vinaraphong and J. McGuire, *J. Colloid Interface Sci.*, 1993, **161**, 325-334.
31. M. Friedel, D. J. Sheeler and J. E. Shea, *J. Chem. Phys.*, 2003, **118**, 8106-8113.
32. Y. Q. Wang, M. Sarkar, A. E. Smith, A. S. Krois and G. J. Pielak, *J. Amer. Chem. Soc.*, 2012, **134**, 16614-16618.
33. C. Loupiac, M. Bonetti, S. Pin and P. Calmettes, *Biochimica et Biophysica Acta (BBA) - Proteins and Proteomics*, 2006, **1764**, 211-216.
34. D. Russo, M. G. Ortore, F. Spinozzi, P. Mariani, C. Loupiac, B. Annighofer and A. Paciaroni, *Biochimica et Biophysica Acta (BBA) - General Subjects*, 2013, **1830**, 4974-4980.
35. R. D. Gougeon, M. Soulard, J. Miehe-Brendle, J. M. Chezeau, R. Le Dred, P. Jeandet and R. Marchal, *J. Agric. Food. Chem.*, 2003, **51**, 4096-4100.
36. C.-N. H. Thuc, A.-C. Grillet, L. Reinert, F. Ohashi, H. H. Thuc and L. Duclaux, *Appl. Clay Sci.*, 2010, **49**, 229-238.
37. G. McKay, H. S. Blair and J. R. Gardner, *J. Appl. Polym. Sci.*, 1982, **27**, 3043-3057.
38. A. K. Bajpai and R. Sachdeva, *J. Appl. Polym. Sci.*, 2000, **78**, 1656-1663.
39. G. V. Joshi, B. D. Kevadiya, H. M. Mody and H. C. Bajaj, *J. Polym. Sci. Part A: Polym. Chem.*, 2012, **50**, 423-430.
40. M. Reinholdt, J. Miehe-Brendle, L. Delmotte, M. H. Tuilier, R. le Dred, R. Cortes and A. M. Flank, *Eur. J. Inorg. Chem.*, 2001, 2831-2841.
41. A. Junghans, C. Champagne, P. Cayot, C. Loupiac and I. Köper, *Langmuir*, 2010, **26**, 12049-12053.
42. L. Liang, H. A. Tajmir-Riahi and M. Subirade, *Biomacromolecules*, 2007, **9**, 50-56.
43. E. Oldfield and A. Allerhand, *J. Amer. Chem. Soc.*, 1975, **97**, 221-224.